

# Chandra X-Ray Point Sources, including Supernova 1979C, in the Spiral Galaxy M100

Philip Kaaret

*Harvard-Smithsonian Center for Astrophysics, 60 Garden St., Cambridge, MA 02138, USA*

pkaaret@cfa.harvard.edu

## ABSTRACT

Six x-ray point sources, with luminosities of  $4 \times 10^{38} - 2 \times 10^{39}$  ergs s<sup>-1</sup> in the 0.4–7 keV band, were detected in Chandra observations of the spiral galaxy M100. One source is identified with supernova SN 1979C and appears to have roughly constant x-ray flux for the period 16–20 years after the outburst. The x-ray spectrum is soft, as would be expected if the x-ray emission is due to the interaction of supernova ejecta with circumstellar matter. Most of the other sources are variable either within the Chandra observation or when compared to archival data. None are coincident with the peak of the radio emission at the nucleus. These sources have harder spectra than the supernova and are likely x-ray binaries. M100 has more bright x-ray sources than typical for spiral galaxies of its size. This is likely related to active star formation occurring in the galaxy.

*Subject headings:* galaxies: individual (NGC 4321 = M100) — galaxies: spiral — galaxies: starburst — supernovae: individual: SN 1979C (M100) — X-rays: galaxies — X-rays: sources

## 1. Introduction

M100 (NGC 4321) is a ‘grand-design’ late-type spiral, which has hosted 4 supernovae since 1900, has a prominent, star-forming circumnuclear region, and is located in the Virgo cluster. Previous x-ray observations of M100 led to the detection of the most recent supernova in the galaxy (SN 1979C) and of a number of other point sources (Immler et al. 1998; Palumbo et al. 1981).

Here, we report on x-ray point sources found in high-angular resolution x-ray observations of M100 made with Chandra. Results on the nuclear emission from the same data were previously reported in Ho et al. (2001). We selected this galaxy for study because it is seen nearly face-on which reduces ambiguity in determining the environments of x-ray sources, because it contains SN 1979C which was previously detected in x-rays (Immler et al. 1998), and because of the question of the association of an x-ray source with the nucleus remains open (Ho et al. 2001). We describe the Chandra observations and our analysis in §2

and discuss the results in §3.

## 2. Observations and Analysis

M100 was observed with the Chandra X-Ray Observatory (CXO; Weisskopf 1988) on 6 Nov 1999 and 15 Jan 2000 using the ACIS spectroscopic array (ACIS-S; Bautz et al. 1998) in imaging mode and the High-Resolution Mirror Assembly (HRMA; van Speybroeck et al. 1997). The galaxy fits almost completely on the S3 chip with a small portion of the  $D_{25}$  ellipse on the S2 chip. We found no point sources within the portion of the  $D_{25}$  ellipse on the S2 chip and the analysis below includes only data from S3. Level 2 data products from the standard processing (version R4CU5UPD11.2) were used. The processing includes standard cuts on CCD event grades, elimination of events from hot pixels, hot columns, and near node boundaries, and removal of cosmic ray induced events.

The observation on 6 Nov 1999 lasted 1165 s and had a high background rate in S3, 10 –

TABLE 1  
CHANDRA X-RAY POINT SOURCES IN M100.

Source	RA	DEC	$\log(L_X)$	Color	Obs 1	Obs 2
C1	12 22 54.78	+15 49 18.3	39.1(1)	-0.2(2)	39.3(1)	38.6(2)
C2	12 22 54.13	+15 49 11.9	39.1(1)	-0.1(2)	38.9(2)	39.2(1)
C3	12 22 54.76	+15 49 15.9	39.0(1)	0.4(3)	39.0(1)	39.0(1)
C4	12 22 54.23	+15 49 43.8	38.8(1)	0.2(3)	38.6(2)	38.9(2)
C5	12 22 58.66	+15 47 51.0	38.9(1)	-0.5(3)	38.9(2)	38.8(2)
C6	12 22 46.10	+15 48 49.7	38.9(1)	0.6(3)	39.1(1)	38.5(3)

NOTE.—This Table contains for each source: Source – the label used in this paper; RA and DEC – the J2000 position;  $\log(L_X)$  – the logarithm of the luminosity in the 0.4–7 keV band in units of  $\text{ergs s}^{-1}$ ; Color – an x-ray color (hardness ratio) defined as counts in the 1–7 keV band minus counts in the 0.4–1 keV band divided by the total counts in the 0.4–7 keV band; Obs 1 and Obs 2 – logarithms of the luminosities in the first and second Chandra observations. Numbers in parentheses indicate the  $1\sigma$  uncertainty in the final digit of the preceding value.

70  $\text{cts s}^{-1}$ . On 15 Jan 2000, 1366 s of data were obtained with a low background rate,  $\sim 1 \text{ cts s}^{-1}$ . Both observations are recorded in Chandra ObsID 400. We created images in the 0.4–7 keV band at the full ACIS resolution of  $0.49''$  for each observation and for the combined data. We searched the images for point sources using wavdetect (CIAO V2.0) and visually inspected each image. For the two sources near the nucleus of M100, wavdetect reported source ellipses well in excess of the HRMA/ACIS point spread function. These large source ellipses are likely due to diffuse emission in this region and we chose to use source regions consistent with the point spread function rather than those reported by wavdetect.

The merged list of sources with detection significance above  $4\sigma$  and within the  $D_{25}$  ellipse of M100 is given in Table 1. The positional accuracy is limited by the Chandra absolute aspect which is accurate to  $0.6''$  ( $1\sigma$  rms; Aldcroft et al. 2000; see also the Chandra Aspect web pages <http://asc.harvard.edu/mta/ASPECT/>). The relative positions should be somewhat better. For each source, counts from the full data set in the energy bands 0.4–1–7 keV were extracted from

source regions with a radius of 2 pixels for sources near the aimpoint and larger elliptical regions for sources further out. The counts were background subtracted using a circular background regions with radii equal to 3 times the major axis of the source ellipse and with ellipses twice the size of the source regions excluded (for both the source of interest and any sources overlapping the background region). For each source, we calculated the x-ray count rate in the 0.4–7 keV band and an x-ray color (hardness ratio) defined as counts in the 1–7 keV band minus counts in the 0.4–1 keV divided by the total counts in the 0.4–7 keV band. The x-ray colors were corrected to the values which would have been measured at the aimpoint using exposure maps for 0.7 and 2.4 keV, which correspond to the average photon energies for the point sources in the two bands.

Count rates were converted to luminosities in the 0.4–7 keV band assuming a thermal bremsstrahlung model with  $kT = 2 \text{ keV}$  and corrected for absorption along the line of sight with a column density of  $2.39 \times 10^{20} \text{ cm}^{-2}$  and assuming a distance of 16.1 Mpc (Ferrarese et al. 1996). The count rates were corrected for the fraction

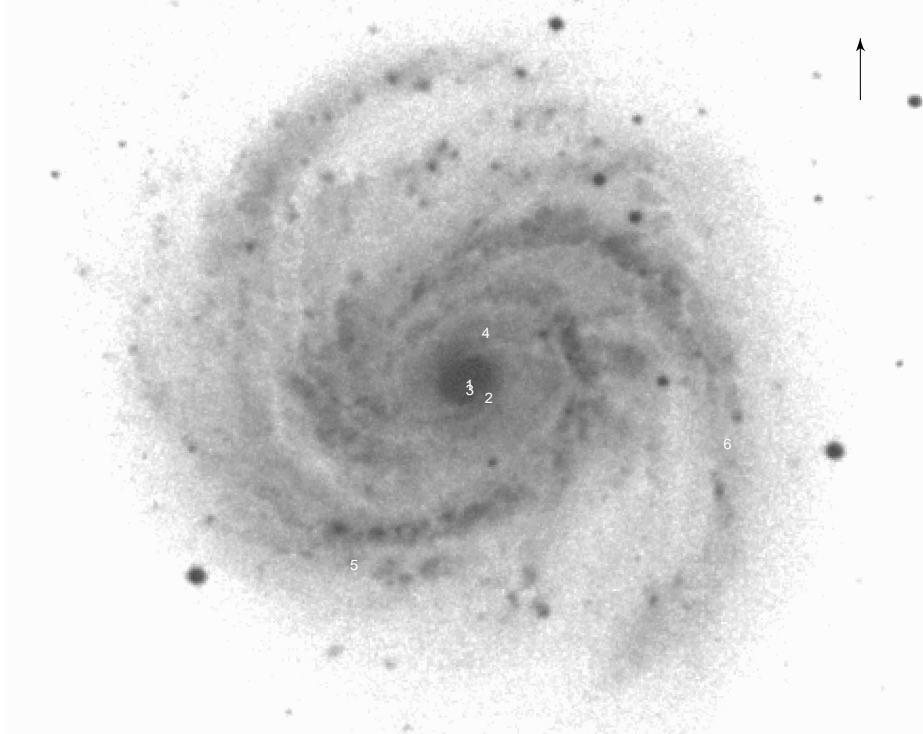


Fig. 1.— B-band image of M100 with positions of the Chandra point sources superimposed. The numbers indicate x-ray sources from Table 1. The arrow points North. The image is from the Digitized Sky Survey.

of events contained in the extraction region and for exposure using an exposure map for 1.5 keV. The  $kT = 2$  keV thermal bremsstrahlung spectrum is consistent with the x-ray colors for most of the sources (see below). The previously used  $kT = 5$  keV thermal bremsstrahlung spectrum (Immler et al. 1998) is not consistent with the x-ray colors. However, use of  $kT = 5$  keV would increase the luminosities only by a factor of 1.3. Use of a power-law with photon index 2 would increase them by 1.1. For comparison with Rosat measurements (Immler et al. 1998), the luminosities in Table 1 should be multiplied by 1.0 to find the equivalent luminosity in the 0.1–2.4 band assuming a thermal bremsstrahlung model with  $kT = 5$  keV for a distance of 17.1 Mpc.

### 3. Results and Discussion

Table 1 gives the properties of the x-ray point sources detected with Chandra. Fig. 1 shows the locations of the Chandra sources superimposed on a Digitized Sky Survey Blue image of

M100. The Chandra sources lie either on spiral arms, in HII regions near spirals arms, or near the nucleus, i.e. at regions of active star formation. This supports the idea that luminous x-ray sources ( $L_X > 2 \times 10^{38}$  ergs  $s^{-1}$ ) are preferentially associated with recent star formation (Fabbiano 1989; Fabbiano et al. 2001).

Comparing the sources detected with Chandra with those detected with Rosat and Einstein (Immler et al. 1998), we find several variable sources. Allowing for the uncertainty in the luminosity due to the lack of spectral information, we require a factor of  $\sim 2$  change as evidence of variability. The Chandra source C6 was undetected with Rosat and appears to have increased in flux by a factor of at least 3. The Chandra upper bound on the luminosity of the Rosat source H17 (Immler et al. 1998) is at least a factor of 4 below the Rosat measurement. The Rosat source H24 appears to have decreased in flux by a factor of at least 2 in the Chandra observation. The source C2 = H21 may also be variable, but caution is warranted before reaching this conclusion as the Rosat

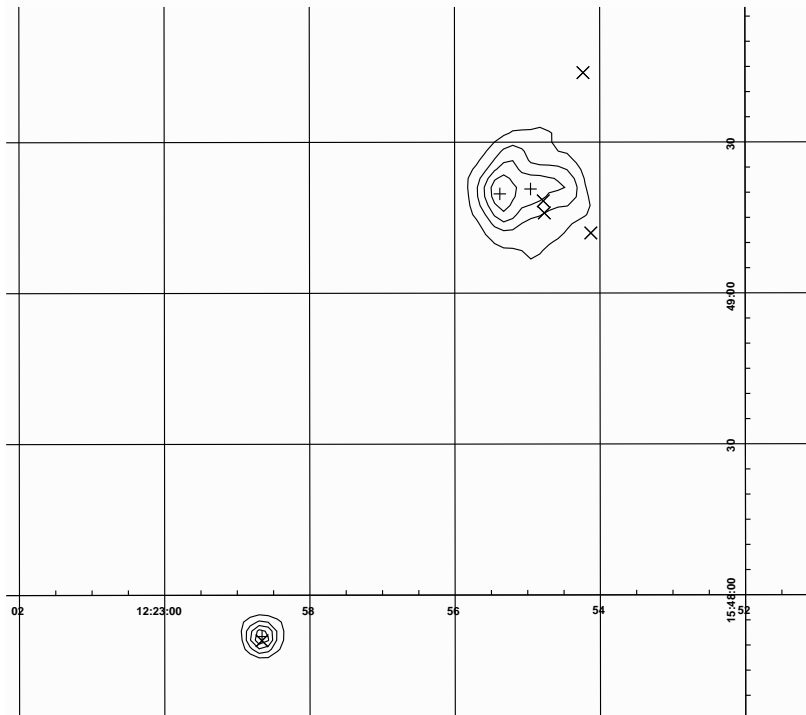


Fig. 2.— Contour map of 1.4 GHz radio emission from M100. The contours are at 1, 2, 3, 4 mJy/beam. Crosses indicate positions of sources from the FIRST catalog and X's indicate x-ray sources from Table 1. The radio emission towards the upper-right is near the nucleus while the emission towards the lower-left is from SN 1979C.

flux may include some diffuse emission due to the larger point spread function of Rosat. This source was also detected with Einstein at a comparable flux. The Rosat sources H18 and H19 were detected at lower fluxes (the Rosat observation was 43 ks compared to only 2.5 ks for Chandra) and their variability cannot be constrained from the short Chandra observation. A longer Chandra observation would be useful. H19 was detected with Einstein at a much higher flux than with Rosat and is clearly variable. The sources H22 = C4 and H25 = C5 appear constant.

The nucleus of M100 (Rosat source H 23) resolves with Chandra into two sources: C1 and C3. There is also diffuse emission present in the low background image near the two point sources. C1 lies  $2.7''$  away from the nuclear position derived from Digitized Sky Survey images which has an uncertainty of  $1.7''$  (Cotton et al. 1999). To further investigate association of the C1 with the nucleus, we examined the FIRST radio survey data

at 1.4 GHz for M100 (Becker et al 1995). The FIRST catalog (White et al 1997) contains two sources inside a region of extended emission near the nucleus, see Fig. 2. C1 is not coincident with either FIRST source and lies outside the peak of the diffuse emission. C1 lies  $3.5''$  away from the closer FIRST source (which lies within the optical nuclear error box). The offset between C1 and the FIRST source is significantly larger than the astrometric uncertainty of Chandra of  $1.0''$  at 90% confidence and the uncertainty of the FIRST position which is less than  $0.5''$  at 90% confidence. The FIRST and Chandra positions for SN 1979C, see below, agree within  $0.84''$  indicating there are no gross errors in the x-ray positions. Hence, we exclude an identification of C1 with the bright radio sources near the nucleus of M100. We note that M100 does not show evidence for AGN activity at other wavelengths (Sakamoto et al. 1995).

C1 is the only source which shows significant variability between the two Chandra observations.

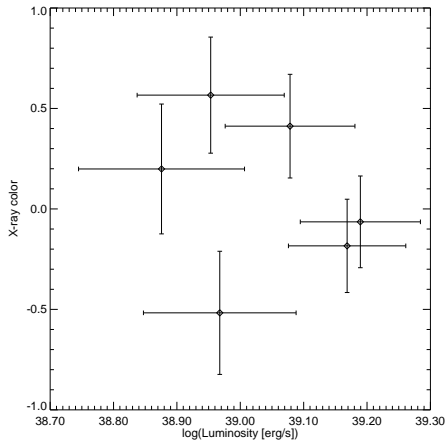


Fig. 3.— X-ray color versus luminosity for point sources in M100.

The variability indicates the source is likely a compact object. The circumnuclear region of M100 is undergoing vigorous star formation with some star clusters as young as a few 10 Myr (Ryder and Knapen 1999). Hence, the presence of bright x-ray point sources near the nucleus is not unexpected and is likely related to the young stellar population.

The majority of the x-ray sources in M100 are variable and are likely x-ray binaries. The sources are not more luminous than known x-ray binaries within the Milky Way, e.g. 4U 1543–47 (Orosz et al. 1998). Hence, they may be normal stellar black hole candidates x-ray binaries with black masses near  $10 M_{\odot}$  and, perhaps, mildly beamed. The luminosities are not high enough to warrant the application of exotic models as may be required for very high luminosity sources, e.g. the  $L_X \sim 10^{41} \text{ erg s}^{-1}$  source in M82 (Kaaret et al. 2001; Matsumoto et al. 2001). In Fig. 3, we show the x-ray color versus x-ray luminosity (both defined in Table 1) of the Chandra sources. Excluding the softest source, which is a supernova discussed below, the colors lie in the range from  $-0.2$ , corresponding to a thermal bremsstrahlung spectrum with  $kT \sim 1.0 \text{ keV}$  or a power-law spectrum with photon index  $\alpha = 2.3$ , to  $+0.6$ , corresponding to  $kT \sim 2.3 \text{ keV}$  or  $\alpha = 0.6$ , assuming a column density of  $2.39 \times 10^{20} \text{ cm}^{-2}$ . Such spectra are reasonable for accreting x-ray binaries at these luminosities.

Using the x-ray point source luminosity function derived from a Rosat survey of nearby spiral galaxies (Roberts and Warwick 2000), we estimate that roughly 1.4 x-ray sources with  $L_X \geq 5 \times 10^{38} \text{ erg s}^{-1}$  would be expected in M100 given its blue luminosity. We find 6 sources. The number of x-ray point sources versus blue luminosity in M100 is similar to that found for M101 (Wang, Immler, and Pietsch 1999) and is likely related to active star formation, as has been suggested for M101 (Trinchieri, Fabbiano, and Romaine 1990). Star formation in M100 is concentrated along the spiral arms (Knapen et al. 1996) as are the Chandra sources.

### 3.1. SN 1979C

The Rosat source H25 was identified with the supernova SN 1979C (Immler et al. 1998). Our Chandra position places the source C5 only  $0.84''$  away from the supernovae – within the 90% confidence error circle – and greatly strengthens this association. None of the other known supernovae are detected with Chandra. SN 1901B and SN 1959E are type I supernova (Barbon, Cappellaro, and Turatto 1989), so no x-ray emission would be expected (Schlegel 1995). The type of SN 1914A is not known.

Unfortunately, there are too few photons ( $\sim 10$ ) detected with Chandra from SN 1979C to make definitive statements about the spectrum (e.g. whether it is thermal line emission versus continuum emission). The source is the softest of those found in M100. The x-ray color, defined above, of  $-0.5 \pm 0.3$  is consistent with a thermal bremsstrahlung spectrum with  $kT = 0.3 - 1.1 \text{ keV}$ , or a power-law spectrum with photon index of 2.3 to 4.3. This assumes a column density of  $2.39 \times 10^{20} \text{ cm}^{-2}$ ; higher absorption would imply a softer intrinsic spectrum. The spectrum is significantly softer than the assumed spectrum used in calculating luminosities in Table 1 or in Immler et al. (1998). Recalculating the luminosity using a more appropriate spectrum, thermal bremsstrahlung with  $kT = 0.6 \text{ keV}$ , we find a luminosity of  $9 \times 10^{38} \text{ erg s}^{-1}$  in the 0.1–2.4 keV band and a luminosity from the Rosat data of  $1.3 \times 10^{39} \text{ erg s}^{-1}$  in the same band.

The Chandra and Rosat fluxes for the source H25 = C5 are not strongly inconsistent given the uncertainties due to spectral shape and inter in-

strument calibration. The source appears to have had a roughly constant, or perhaps slightly declining, luminosity over the 4.3 years separating the two observations. The constancy of the x-ray luminosity of SN 1979C over 4 years beginning 16 years after outburst is similar to the x-ray light curve of SN 1978K in NGC 1313 which showed a constant luminosity of  $\sim 5 \times 10^{39} \text{erg s}^{-1}$  over the period 12–16 years after outburst (Schlegel et al. 1996).

SN 1979C was discovered on 19 April 1979 near maximum optical light (Johnson 1979) and has been extensively observed. The optical light curve had a linear decline, leading to classification as a type II, subclass ‘L’ or ‘linear’ (Panagia et al. 1980). The total radiative energy in the event was  $7 \times 10^{49} \text{erg}$  (Panagia et al. 1980). The progenitor is thought to be a red supergiant with a mass near  $17 M_{\odot}$  and may have been in a binary (Weiler et al. 1992; Schwarz and Pringle 1996). Hubble Space Telescope (HST) observations led to tentative identification of an optical counterpart to SN 1979C (Van Dyk et al. 1999). The  $\text{H}\alpha$  flux from the counterpart would imply an  $\text{H}\alpha$  to X-ray flux ratio of  $\sim 0.013$  during 1995–1996.

The interaction of supernova ejecta with surrounding matter previously lost by the progenitor provides an adequate explanation of optical, UV, and radio data on SN 1979C (Chevalier and Fransson 1994). Radio emission was detected one year after outburst with the maximum emission at 6 cm shortly after the first detection and the maximum at 20 cm three years after outburst (Weiler et al. 1981, 1986). This delayed turn-on with increasing delay at longer wavelengths appears due to decreasing free-free absorption in ionized gas around the supernova and is well explained by the circumstellar interaction model (Weiler et al. 1991). The same model also explains the observed UV lines (Fransson 1984).

Circumstellar interactions could produce the observed roughly constant luminosity if the supernova ejecta and the circumstellar matter have the appropriate radial dependence (Schlegel et al. 1996). Such a process could produce adequate luminosity and the  $\text{H}\alpha$  to X-ray flux ratio is in reasonable agreement with model predictions (Chevalier and Fransson 1994). A soft x-ray spectrum would be expected, which is consistent with the Chandra constraints. The circumstellar interac-

tion model appears consistent with all the available x-ray constraints.

Alternative explanations of the x-ray emission are possible if a compact object was formed in SN 1979C. The X-ray emission might arise from a rotation-powered pulsar or from accretion on to a compact object fueled either by a binary companion or by matter from the progenitor which has fallen back onto the compact object (Chatterjee et al. 2000). Sufficient flux could be produced by either method of accretion (a black hole would be required to avoid violating the Eddington limit if the emission is unbeamed), but a variable or declining flux and, perhaps, a somewhat harder spectrum than is observed might be expected. The presence of a pulsar in SN 1979C has been suggested to explain the radio light curves (Weiler et al. 1981; Pacini and Salvati 1981). The behavior of very young pulsars is unknown with a key question being the efficiency for conversion of spin-down power to observable x-ray emission. X-rays would likely come mainly from a surrounding synchrotron nebula and produce a relatively hard power-law x-ray spectrum, mildly inconsistent with the Chandra constraints. With additional x-ray observations, it would be possible to search for variability and perhaps also to determine whether the x-ray emission is thermal line emission or due to a continuum process and to accurately measure the spectral parameters.

I gratefully acknowledge the efforts of the Chandra team and partial support from NASA grant NAG5-7405. I thank the referee (and editor) Greg Bothun for useful comments. The Digitized Sky Survey was produced at the Space Telescope Science Institute under U.S. Government grant NAG W-2166.

## REFERENCES

- Aldcroft T.L. et al. 2000, Proc. SPIE, 4012, 650  
 Barbon, R., Cappellaro, E., & Turatto, M. 1989, A&ApS, 81, 421  
 Bautz M.W. et al. 1998, Proc. SPIE, 3444, 210  
 Becker, R.H., White, R.L., & Helfand, D. 1995, ApJ, 453, 741  
 Chevalier, R.A. & Fransson, C. 1994, ApJ, 420, 268

- Chatterjee, P., Hernquist, L., & Narayan R. 2000, *ApJ*, 534, 373
- Colbert E.J.M., Mushotzky R.F. 1999, *ApJ*, 519, 89
- Collura A., Reale F., Schulman E., Bregman J.N. 1994, *ApJ*, 420, L63
- Cotton, W.D., Condon, J.J., & Arbizazani, E. 1999, *ApJS*, 125, 409
- de Vaucouleurs, G., de Vaucouleurs, A., Buta, R., Ables, H.D., & Hewitt, A.V. 1981, *PASP*, 93, 36
- Fabbiano G. 1989, *ARA&A*, 27, 87
- Fabbiano, G. Zezas, A., & Murray, S.S. 2001, *ApJ*, to appear
- Freedman, W.L. et al. 1994, *ApJ*, 435, L31
- Ferrarese, L. et al. 1996, *ApJ*, 464, 568
- Fransson, C. 1994, *A&A*, 133, 264
- Ho, L.C. et al. 2001, *ApJ*, to appear, *astro-ph/0102504*
- Immler, S., Pietsch, W., & Aschenbach, B. 1998, *A&A*, 331, 601
- Johnson, G.E., 1979, *IAU Circ.*, No. 3348
- Kaaret, P., Prestwich, A.H., Zezas, A., Murray, S.S., Kim, D.-W., Kilgard, R.E., Schlegel, E.M., & Ward, M.J. 2001, *MNRAS*, 321, L29
- Knapen, J.H., Beckman, J.E., Cepa, J., & Nakai, N. 1996, *A&A*, 308, 27
- Matsumoto, H., Tsuru, T.G., Koyama, K., Awaki, H., Canizares, C.R., Kawai, N., Matsushita, S., & Kawabe, R. 2001, *ApJ*, 547, L25
- Orosz, J.A., Jain, R.K., Bailyn, C.D., McClintock, J.E., & Remillard, R.A. 1998, *ApJ*, 499, 375
- Pacini, F. & Salvati, M. 1981, *ApJ*, 245, L107
- Palumbo, G.G.C., Maccacaro, T., Panagia, N., Vettolani, G., & Zamorani, G. 1981, *ApJ*, 247, 484
- Panagia, N. et al. 1980, *MNRAS*, 192, 861
- Roberts, T.P. & Warwick, R.S. 2000, *MNRAS*, 315, 98
- Ryder, S.D. & Knapen, J.H. 1999, *MNRAS*, 302, L7
- Sakamoto, K., Okumura, S., Minezaki, T., Kabayashi, Y., & Wada, K. 1995, *AJ*, 110, 207
- Schlegel, E.M. 1995, *Rep. Prog. Phys.*, 58, 1375
- Schlegel, E.M., Petre, R., & Colbert, E.J.M. 1996, *ApJ*, 456, 187
- Schwarz, D.H. & Pringle, J.E. 1996, *MNRAS*, 282, 1018
- Trinchieri, G., Fabbiano, G., & Romaine, S. 1990, *ApJ*, 356, 110
- Van Dyk, S.D. et al. 1999, *PASJ*, 111, 313
- van Speybroeck L.P. et al. 1997, *Proc. SPIE*, 3113, 89
- Wang, Q.D., Immler, S., & Pietsch, W. 1999, *ApJ*, 523, 121
- Weiler, K.W., van der Hulst, J.M., Sramek, R.A., & Panagia, N. 1981, *ApJ*, 243, L151
- Weiler, K.W., Sramek, R.A., Panagia, N., van der Hulst, J.M., & Salvati, M. 1986, *ApJ*, 301, 790
- Weiler, K.W., Van Dyk, S.D., Discenna, J.L., Panagia, N., & Sramek, R.A. 1991, *ApJ*, 380, 161
- Weiler, K.W., Van Dyk, S.D., Pringle, J.E., & Panagia, N. 1992, *ApJ*, 339, 672
- Weisskopf M.C. 1988, *Space Science Reviews*, 47, 47
- White, R.L., Becker, R.H., Helfand, D.J., & Gregg, Michael D. 1997, *ApJ*, 475, 479